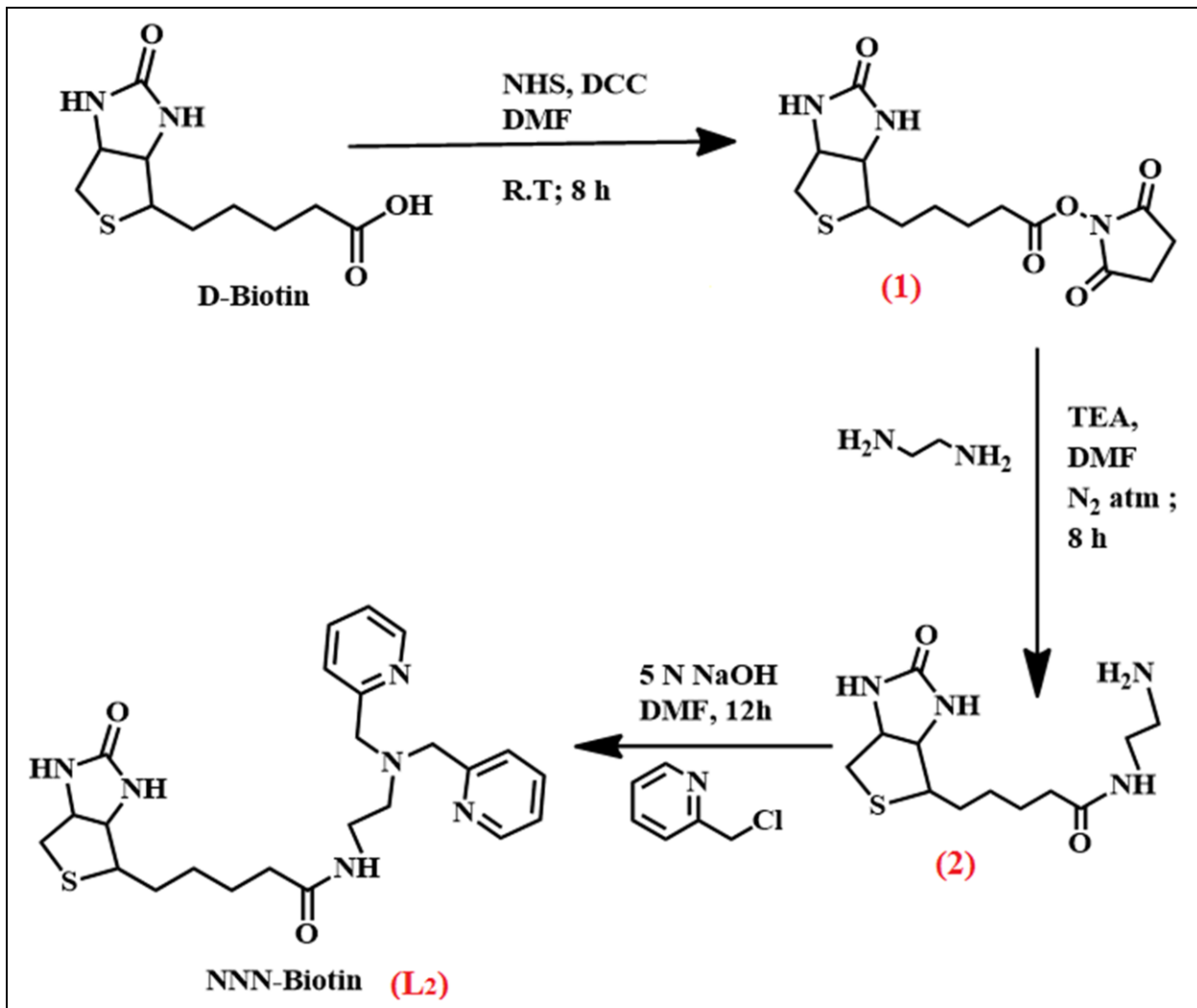


# **European Journal of Inorganic Chemistry**

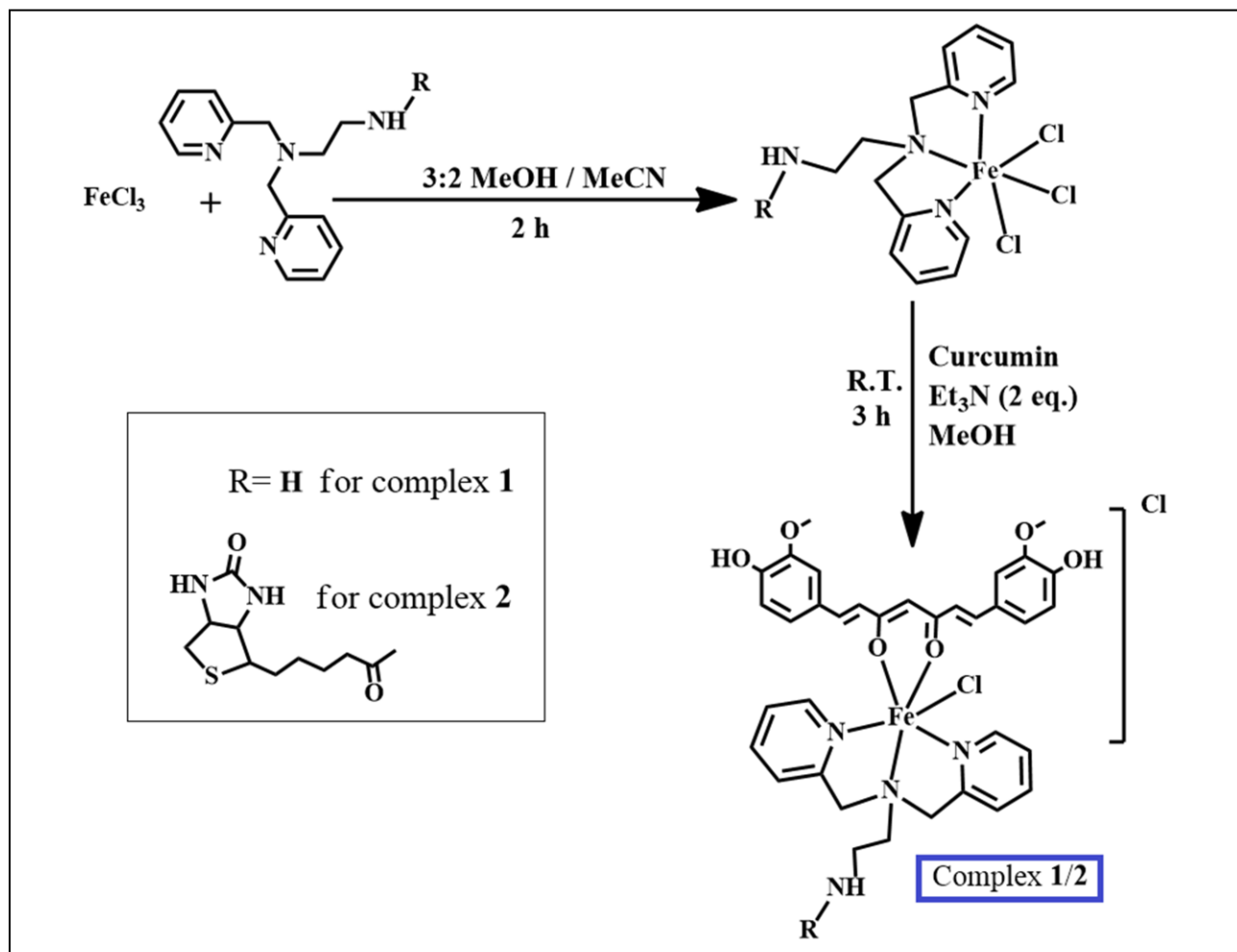
## **Supporting Information**

### **Biotin-Appended Iron(III) Complexes of Curcumin for Targeted Photo-Chemotherapy**

Somarupa Sahoo, Abinaya Raghavan, Arun Kumar, Dipankar Nandi,\* and Akhil R. Chakravarty\*



**Scheme S1.** Synthetic scheme for the preparation of *NNN*-donor biotin-appended dipicolylamine ligand ( $L^2$ ).



**Scheme S2.** Generalized synthetic scheme for the iron(III) complexes **1** and **2**.

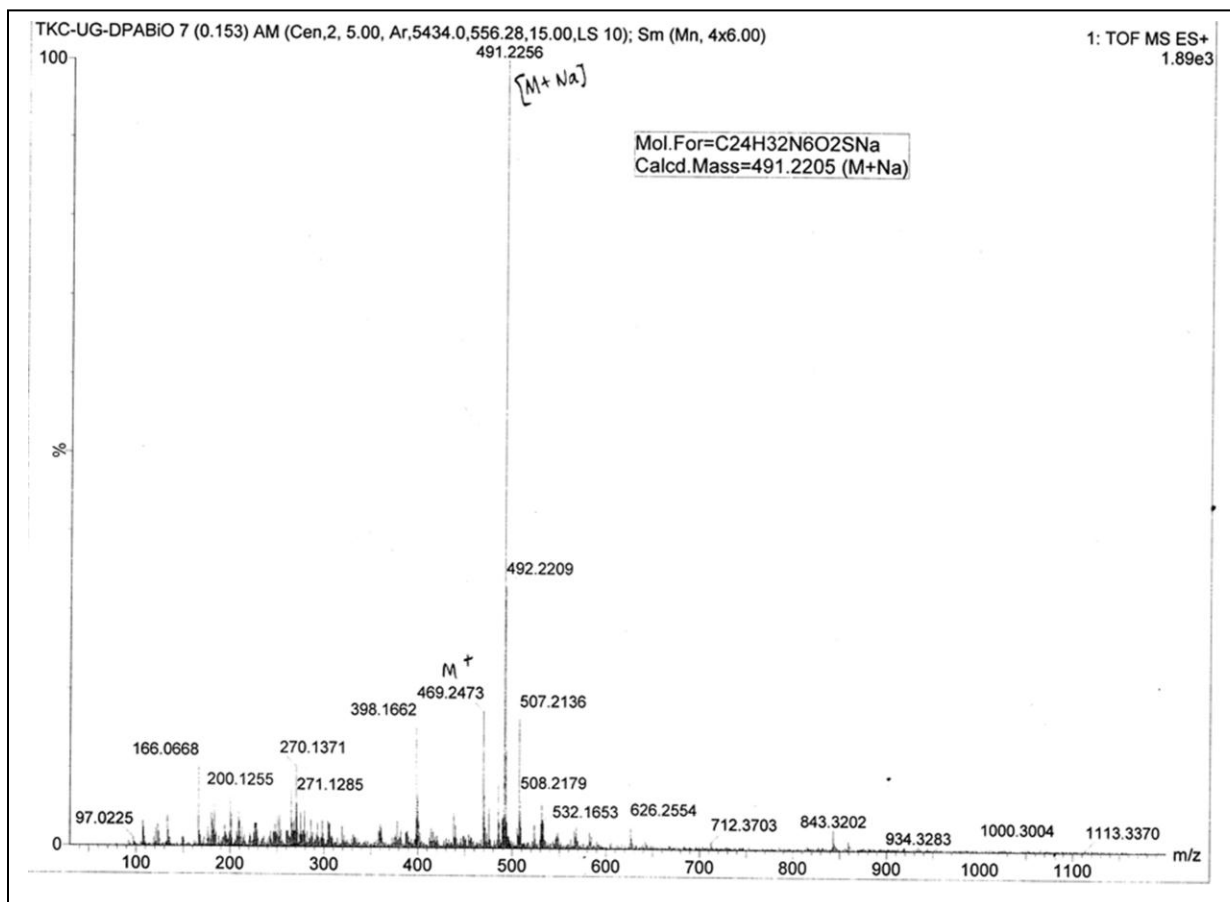


**Figure S1.** ESI-MS spectrum of the biotin ligand ( $L^2$ ) in MeOH showing a prominent peak corresponding to  $[M + Na]^+$  at 491.2256 (m/z).

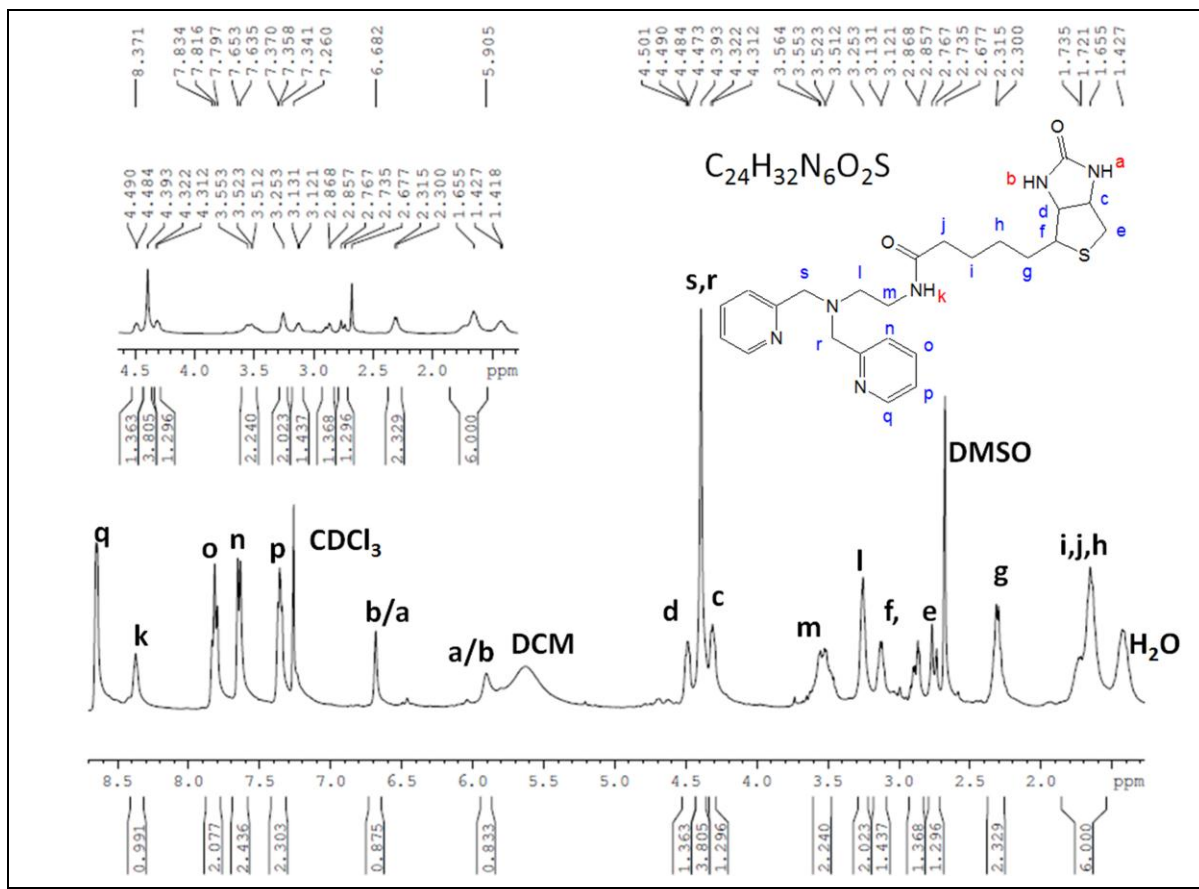


**Figure S2.**  $^1\text{H}$  NMR spectrum of ligand L<sup>2</sup> in  $\text{CDCl}_3$ .

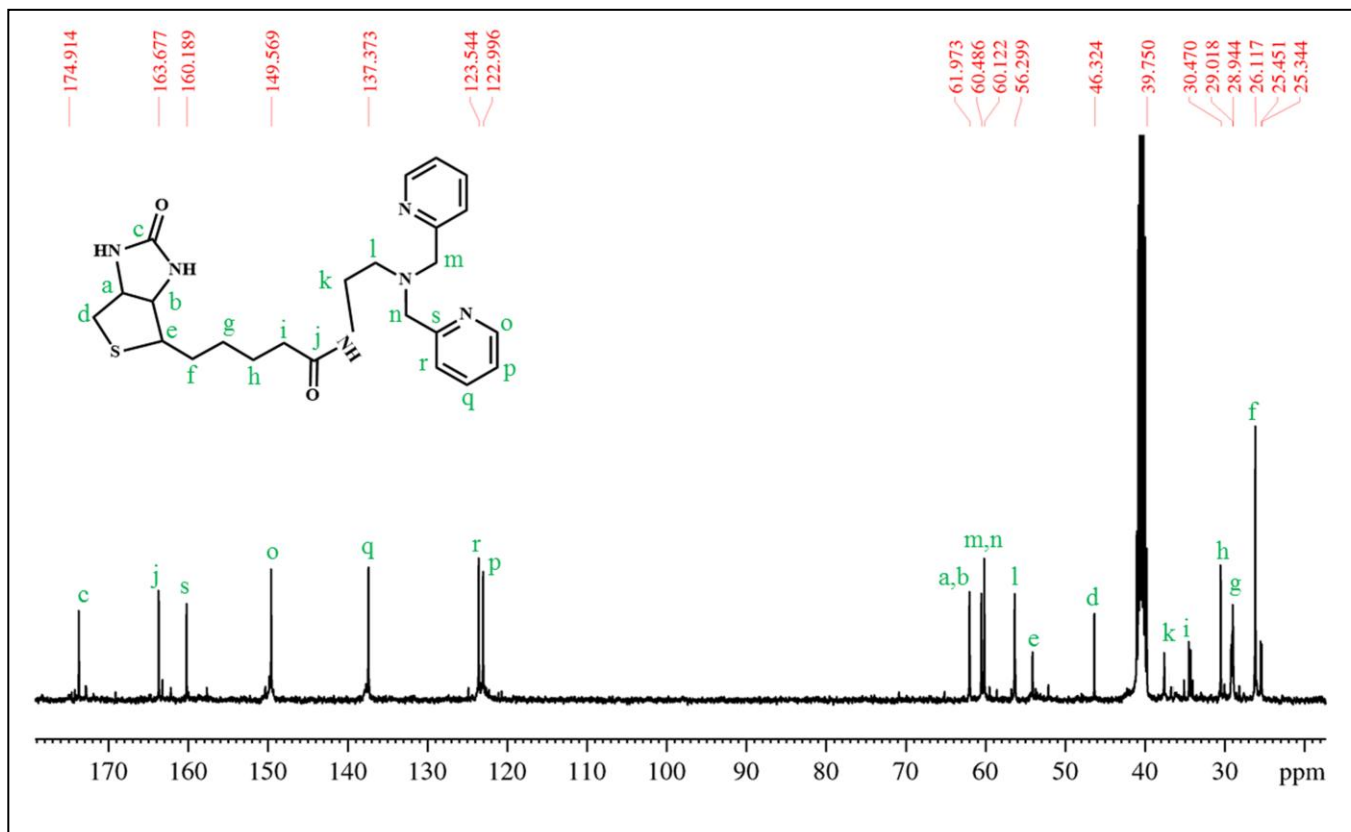


**Figure S3.**  $^{13}\text{C}$  NMR spectrum of ligand  $\text{L}^2$  in  $\text{DMSO-d}_6$ .

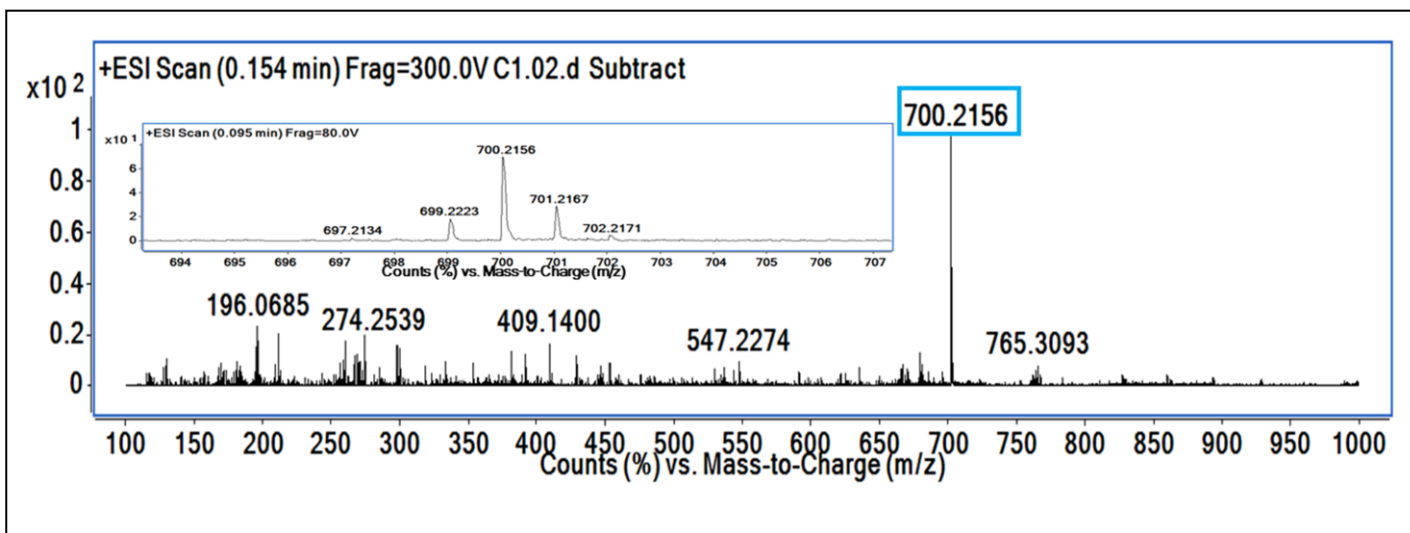


**Figure S4.** ESI-MS spectrum of complex **1** in acetonitrile showing a prominent peak corresponding to  $[\text{M}-\text{Cl}]^+$  at  $700.2156$  ( $m/z$ ). Inset shows the isotopic distribution pattern.

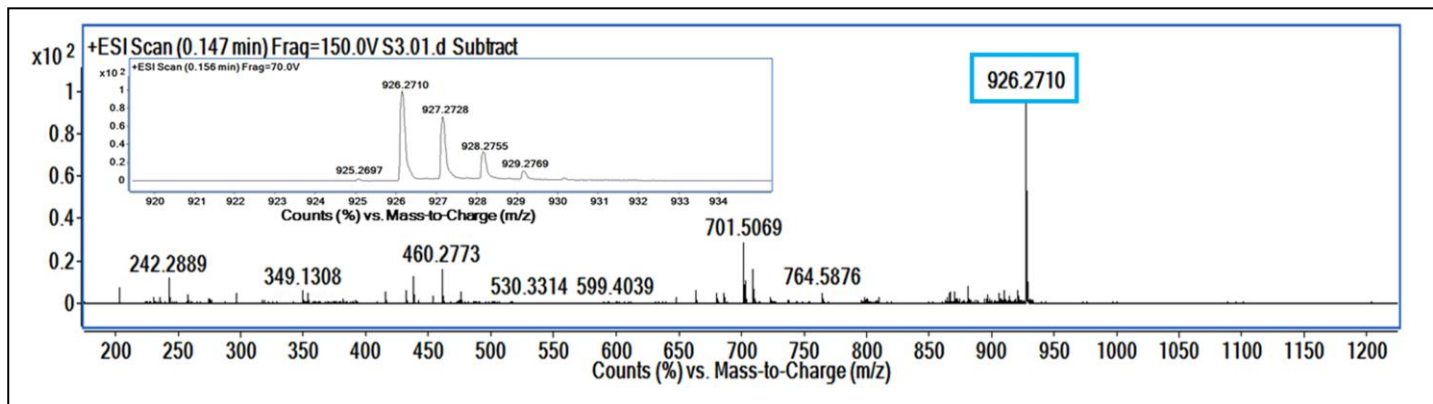


**Figure S5.** ESI-MS spectrum of complex **2** in acetonitrile showing a prominent peak corresponding to  $[M-Cl]^+$  at 926.2710 ( $m/z$ ). Inset shows the isotopic distribution pattern.

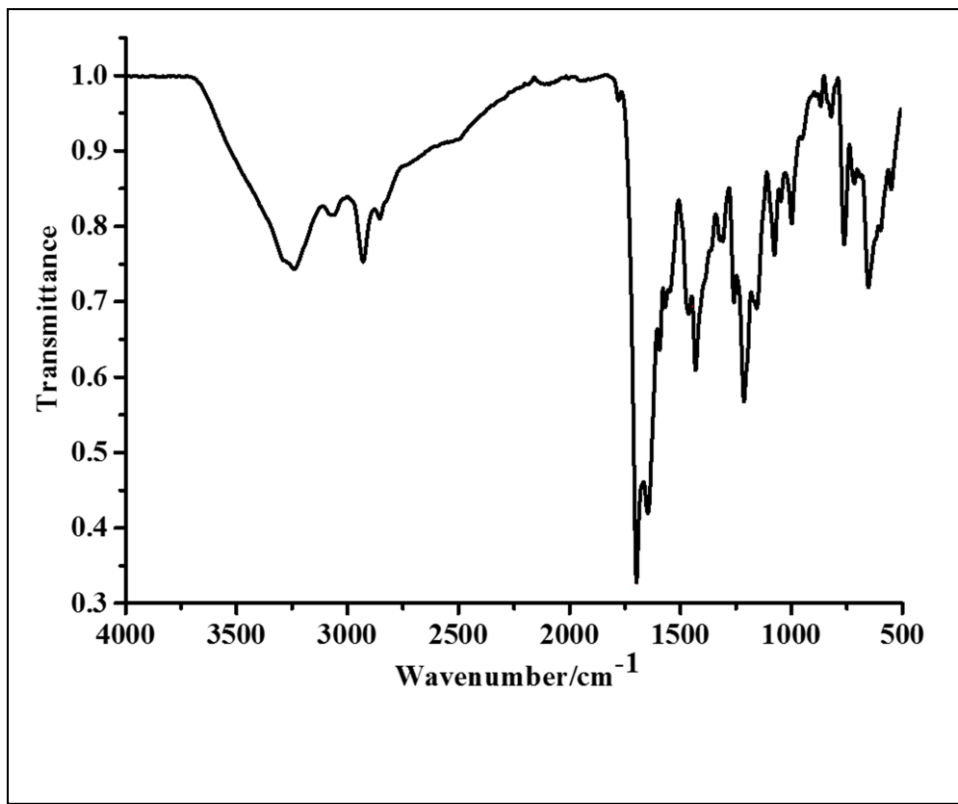


**Figure S6.** IR spectrum of ligand  $L^2$  in the solid phase showing a strong peak for keto the group observed at  $1660\text{ cm}^{-1}$ .

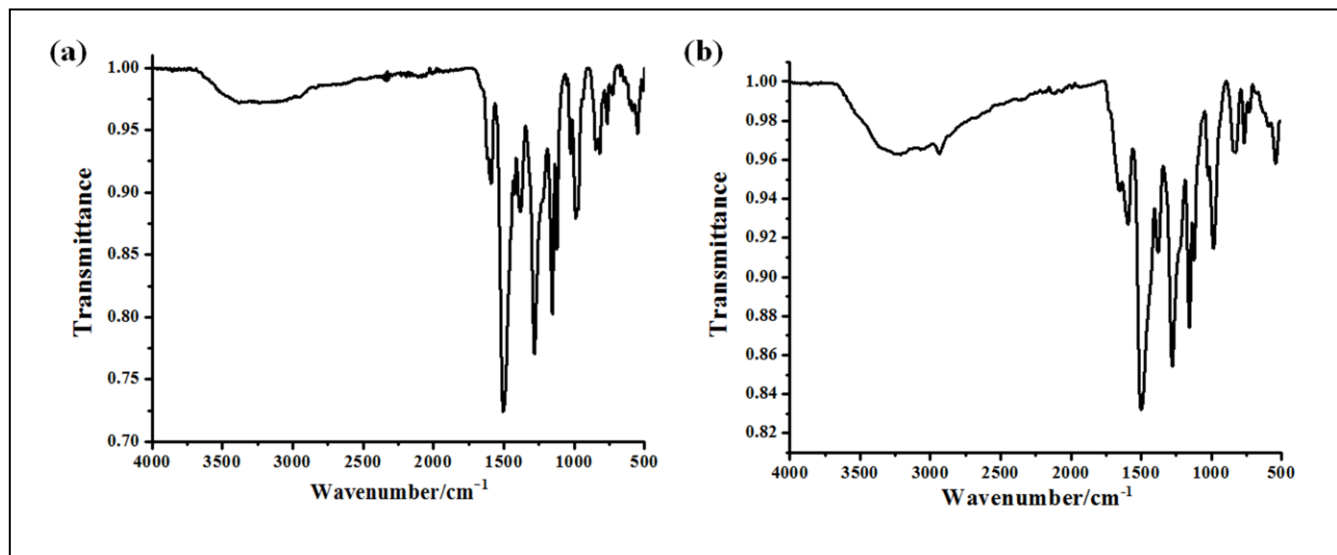


**Figure S7.** IR spectra of the complexes **1** and **2** in the solid phase: **1**, (a); **2**, (b).

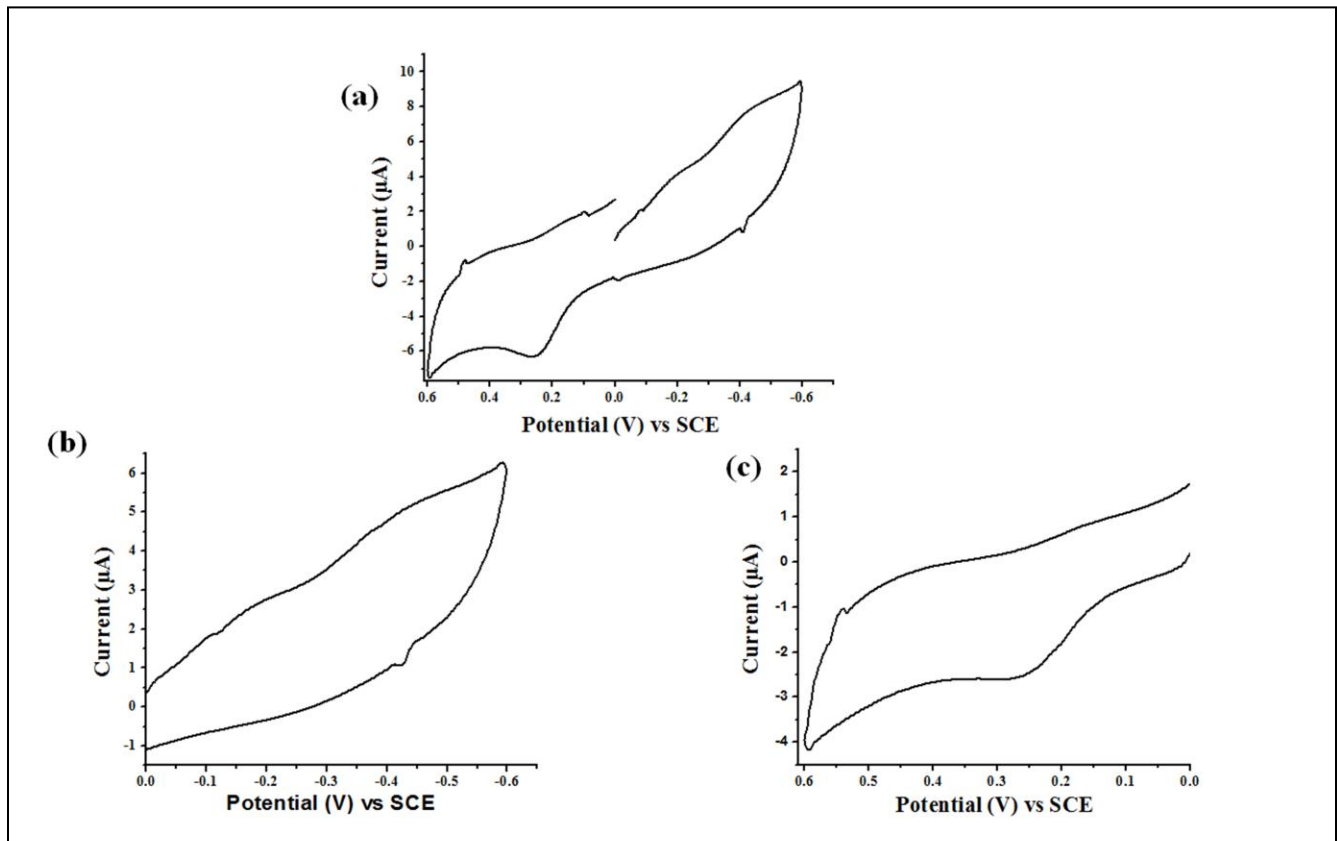


**Figure S8.** Cyclic voltammograms of complex **1** showing the Fe(III)/Fe(II) redox response in 0.1 M TBAP-DMF at a scan rate of 100 mV s<sup>-1</sup> : Full scan, (a); Cathodic scan, (b); Anodic scan, (c). The redox responses are sluggish in nature without showing any reversibility.

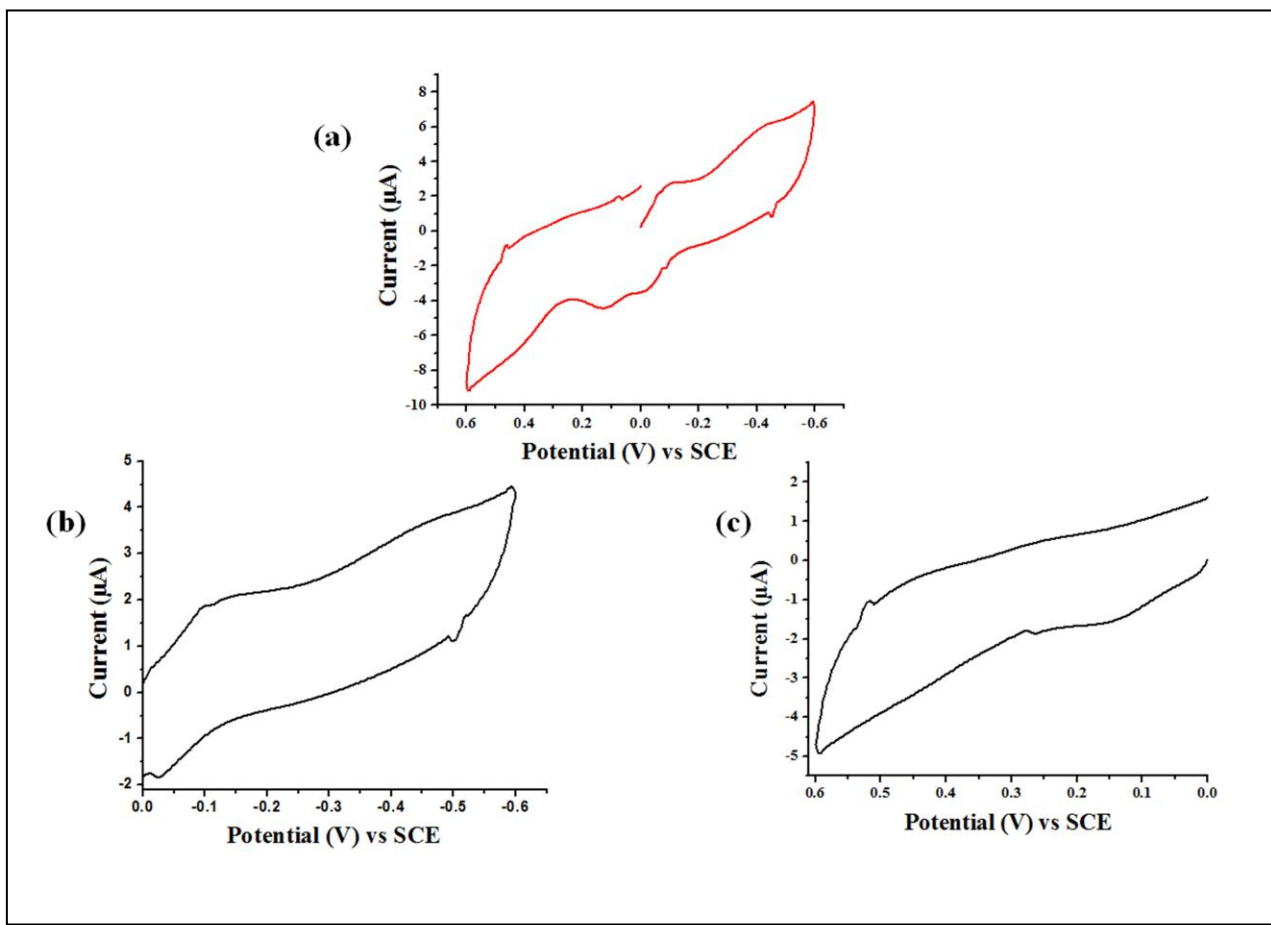


**Figure S9.** Cyclic voltammograms of complex **2** showing the Fe(III)/Fe(II) redox responses in 0.1 M TBAP-DMF at a scan rate of  $100 \text{ mV s}^{-1}$  : Full scan, (a); Cathodic scan, (b); Anodic scan, (c). The redox responses are sluggish in nature.

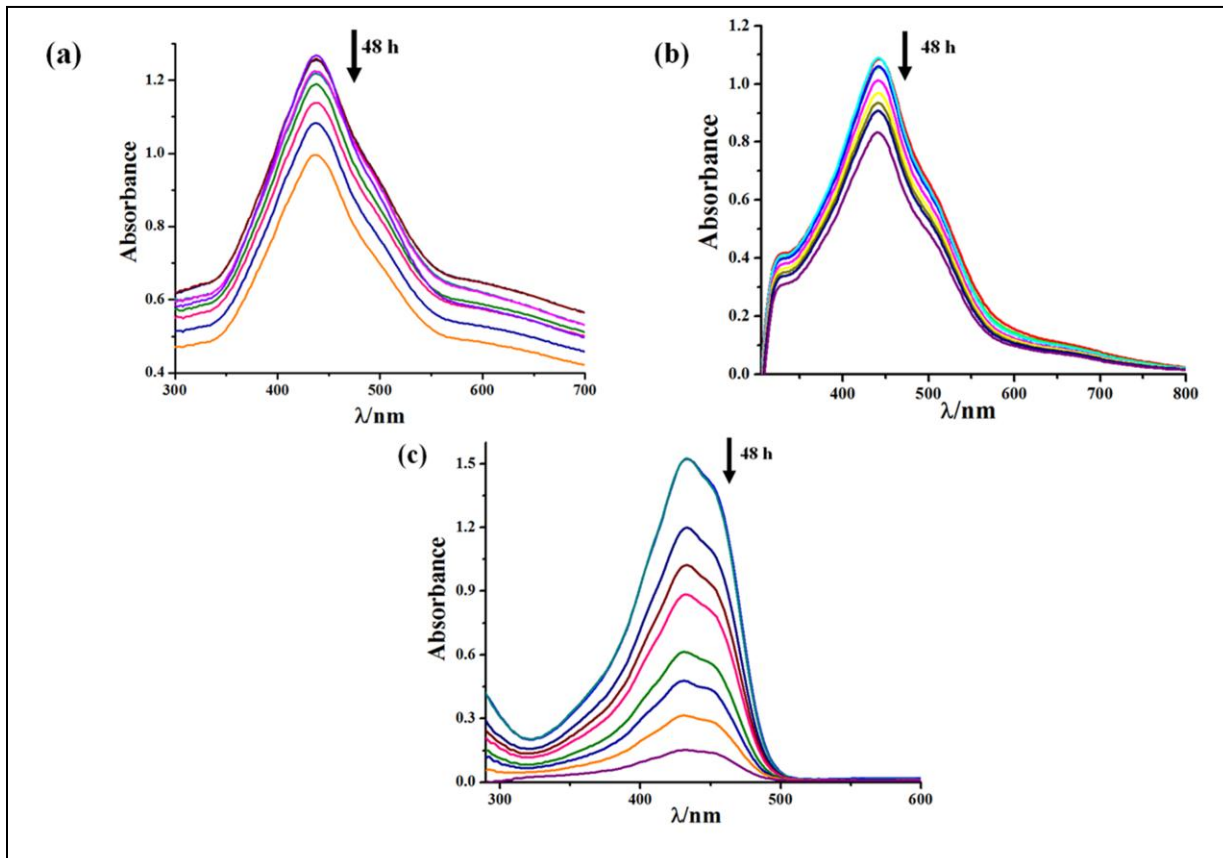


**Figure S10.** The UV-visible spectral traces of the complexes in DMSO/DPBS (1:1 v/v) recorded over a period of 48 h showing very less decrease in the intensity or position of the absorption bands in case of complexes **1** and **2** indicating their excellent stability for about 12 h (a , b). Plot (c) shows gradual and rapid decay of curcumin (HCur) within the same time period indicating its instability in the buffer medium.

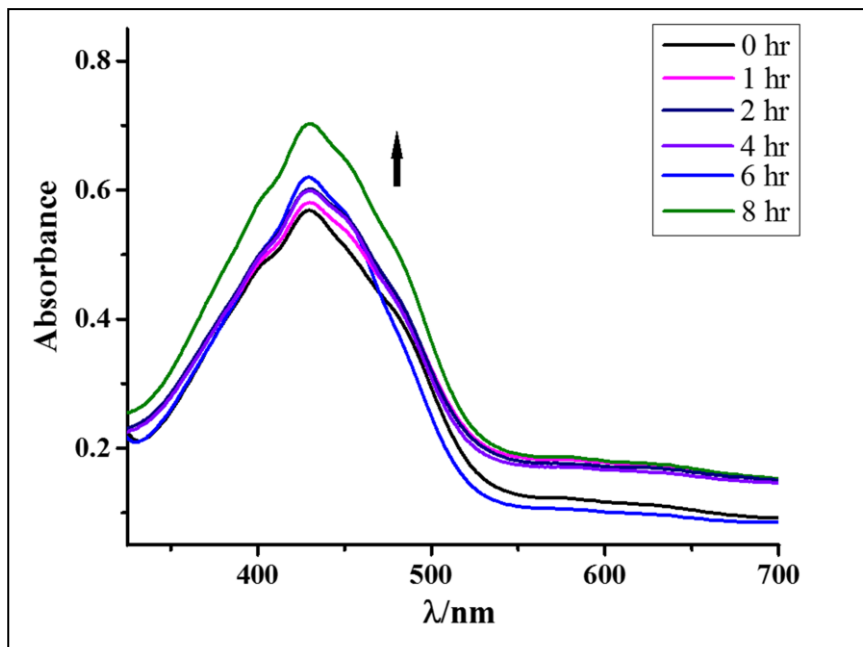


**Figure S11.** The UV-visible spectral traces of complex **2** in 2 % DMSO/DMEM (phenolate red free media; pH: 7.2) recorded over a period of 8 h showing very less decrease in the intensity or position of the absorption bands indicating its stability within the in vitro incubation time of 4 h.

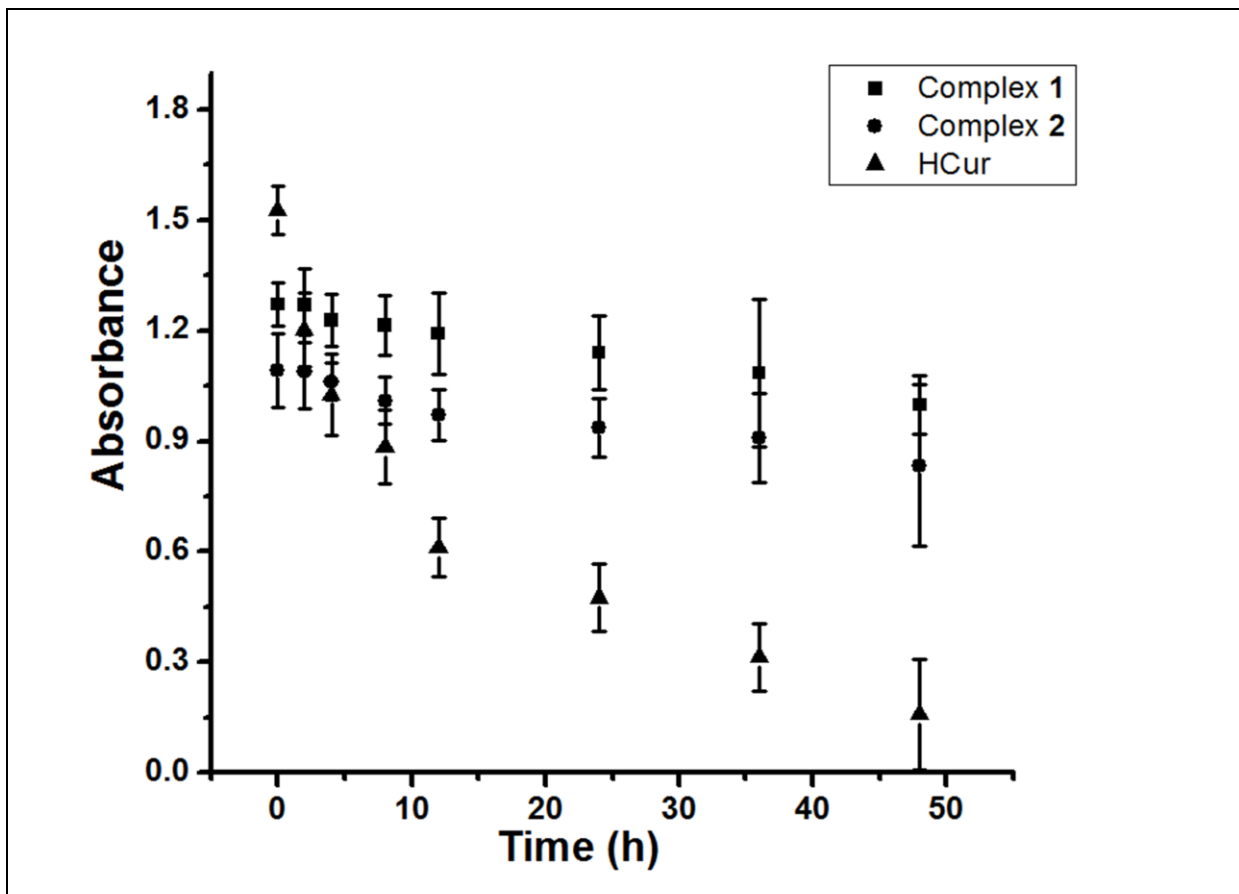


**Figure S12.** Photostability of the complexes and curcumin studied up to 48 h in 1:1 DMSO/DPBS medium upon 1 h irradiation with visible light (400-700 nm) with error bars. The instability of only curcumin is observed from the slope when compared to those of the complexes **1** and **2**.

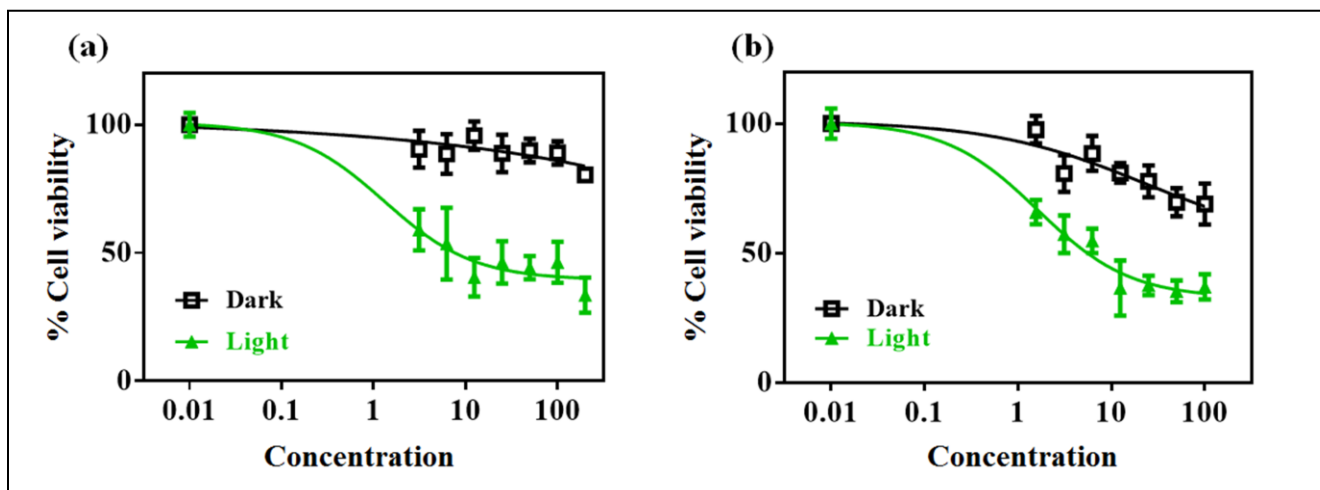


**Figure S13.** Photocytotoxicity of complexes **1** and **2** in HeLa cells upon irradiation with visible light (400- 700 nm,  $10 \text{ J cm}^{-2}$ , green symbol) and in dark (black symbol) after 4 h incubation of the cells with the complexes: **1** (a), **2** (b).

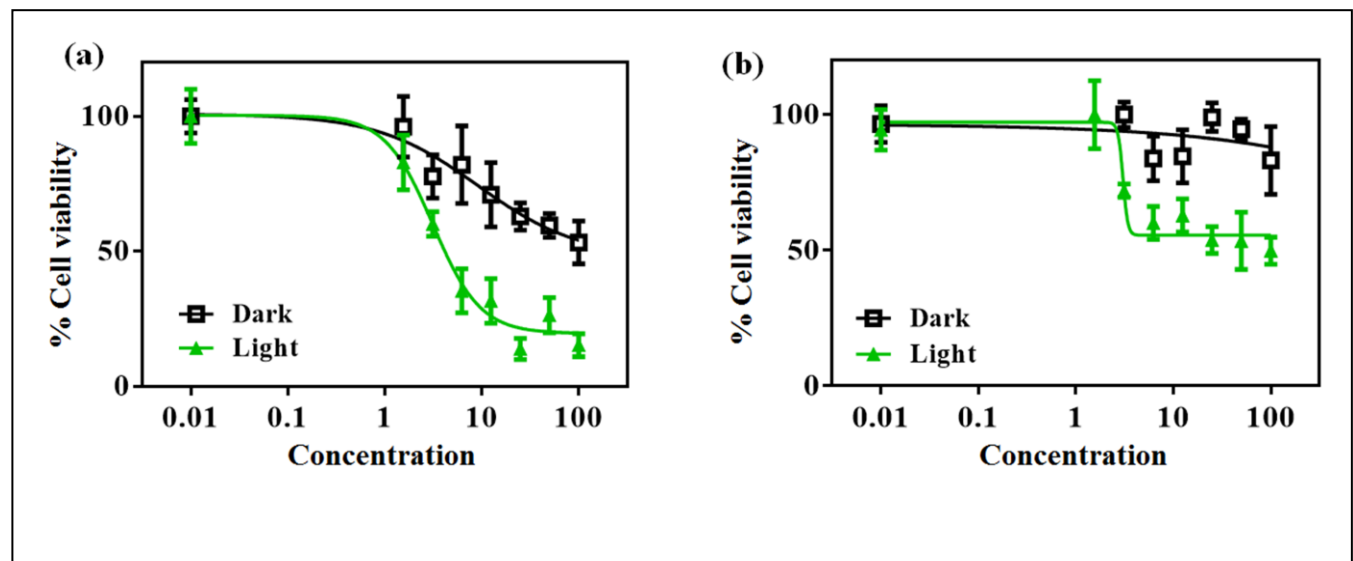


**Figure S14.** Photocytotoxicity of complexes **1** and **2** in MCF-7 cells upon irradiation with visible light (400- 700 nm,  $10 \text{ J cm}^{-2}$ , green symbol) and in dark (black symbol) after 4 h incubation of the cells with the complexes: **1** (a), **2** (b).

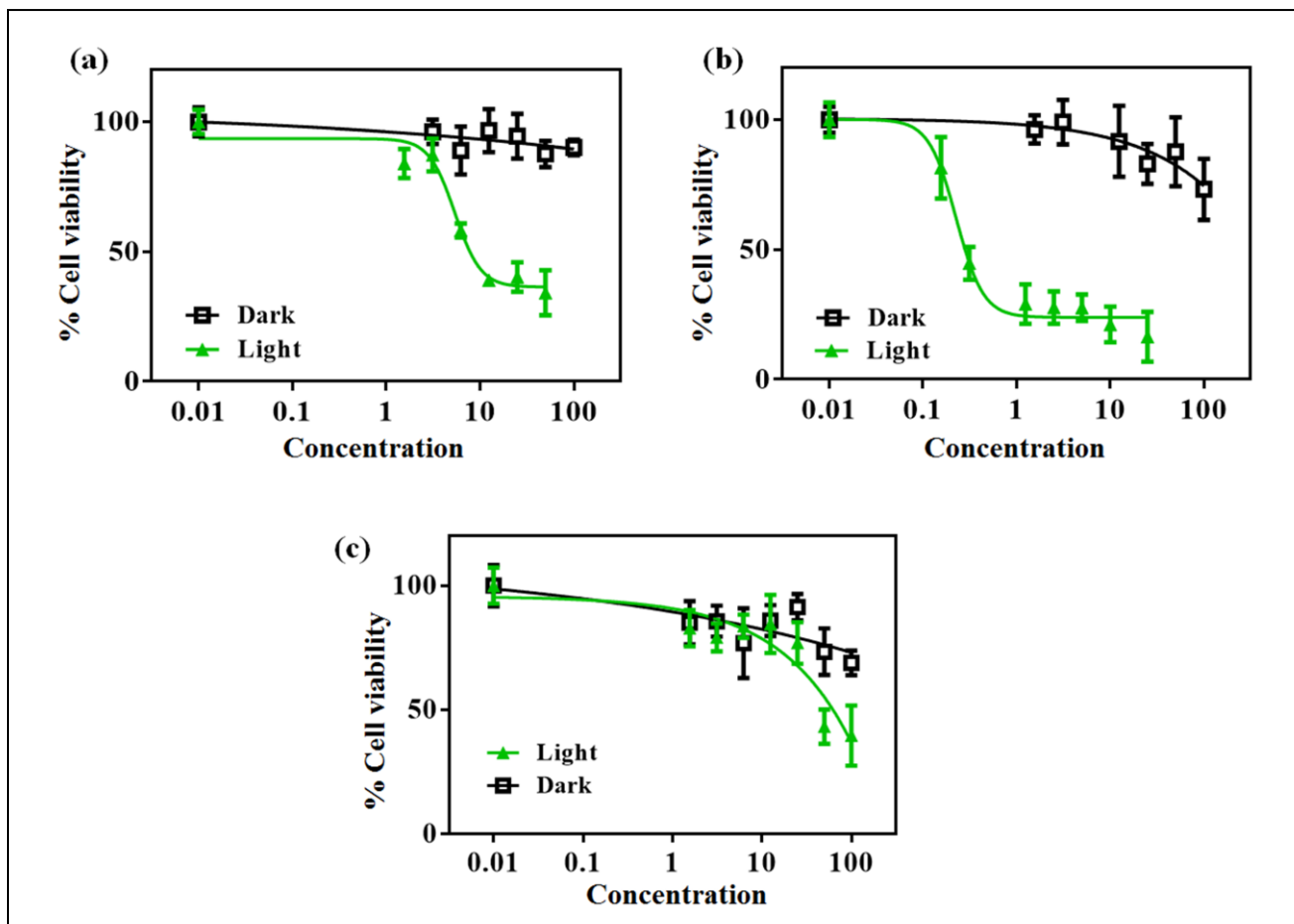


**Figure S15.** Photocytotoxicity of complexes **1** and **2** in HepG2 cells upon irradiation with visible light (400- 700 nm,  $10 \text{ J cm}^{-2}$ , green symbol) and in dark (black symbol) after 4 h incubation of the cells with the complexes: **1** (a), **2** (b).

(c) An increase in the  $\text{IC}_{50}$  value upon saturation with 2 mM biotin (1 h) is shown in this plot. This corresponds to the histogram shown in Figure S14.

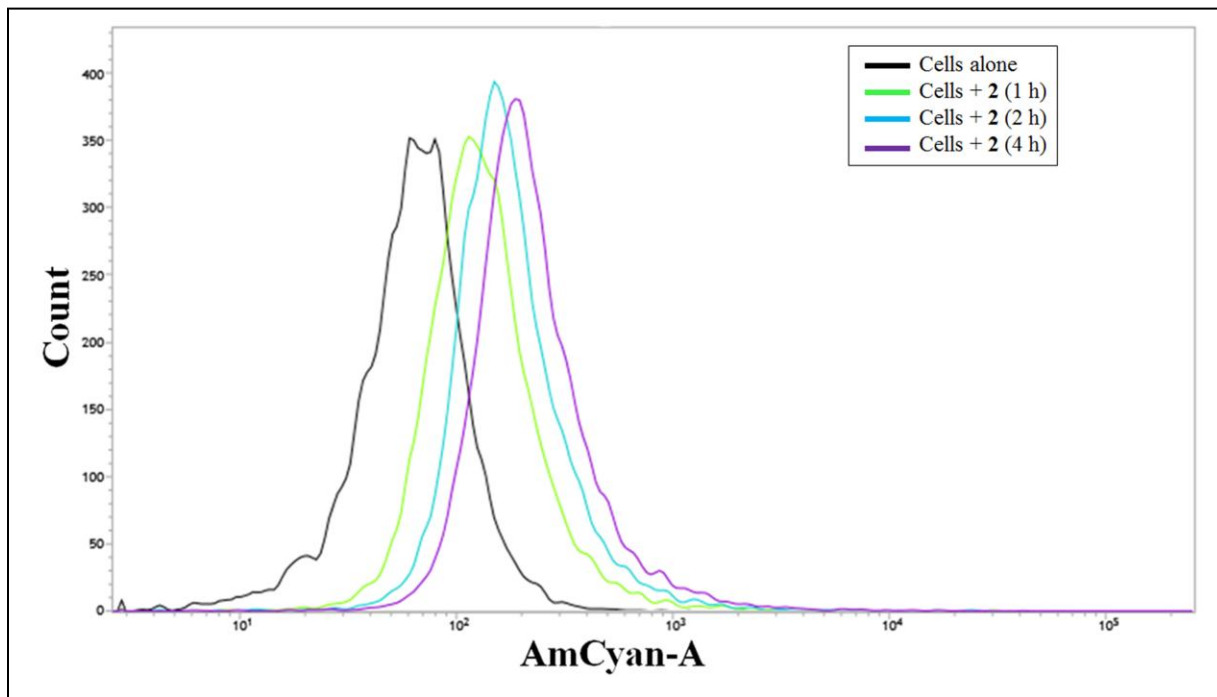


**Figure S16.** Histogram showing time dependent cellular incorporation of complex 2 ( $2 \mu\text{M}$ ) in HeLa cells at 1 h, 2 h and 4 h of incubation time at  $37^\circ\text{C}$ .

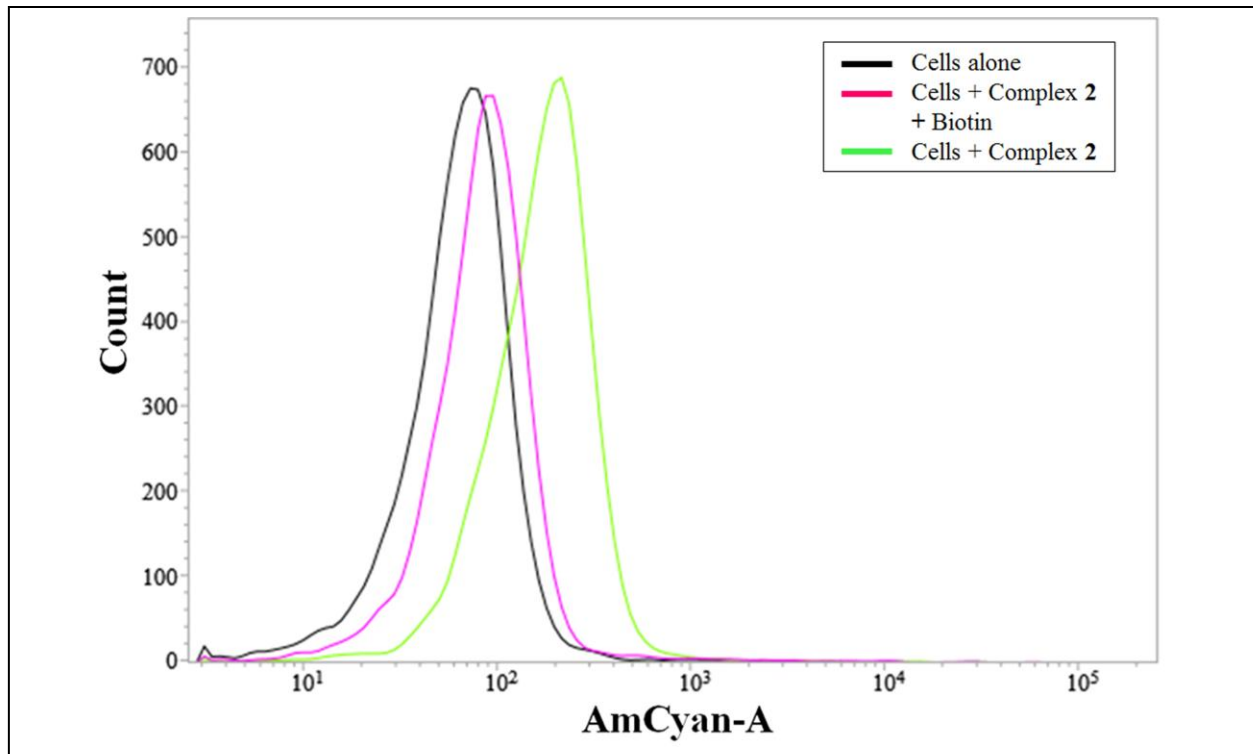


**Figure S17.** Histogram showing effect of pre-saturation with biotin (2 mM) on the cellular incorporation of the complex **2** (2  $\mu$ M) in HepG2 cells at 4 h incubation at 37°C. The uptake is lesser when cells were pre-saturated, as visible in Figure S15 (c) from MTT assay.

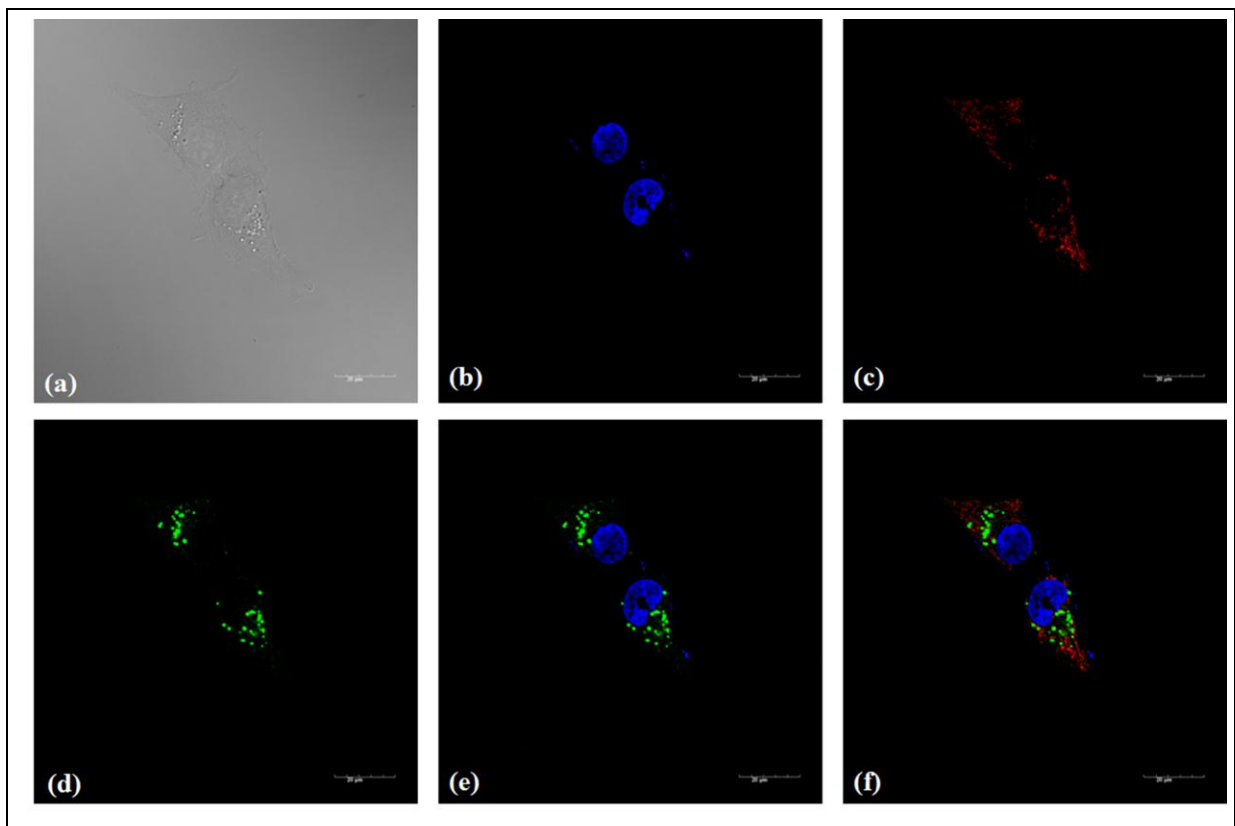


**Figure S18.** Confocal microscopy images of HeLa cells treated with complex **2** ( $20 \mu\text{M}$ ) co-stained with Mito tracker deep red: Panel (a) is bright field; panel (b) is for the blue fluorescence of Hoechst dye which localizes in the cell nucleus; panel (c) is for Mitotracker deep red; panel (d) is for the green fluorescence of complex **2**; panel (e) shows the merged image of (b) and (d) panels indicating non-nuclear localization of the complex; and panel (f) shows the merged image of the panels (b), (c) and (d) (Scale bar =  $20 \mu\text{m}$ ); Magnification: 100 X ; PCC: 0.35. This PCC value indicates only moderate localization of the complex in the mitochondria and non-nuclear localization.

Panels (a) to (d) of this figure are the same and reproduced from Figure 9 of the main text for clarity and comparison.

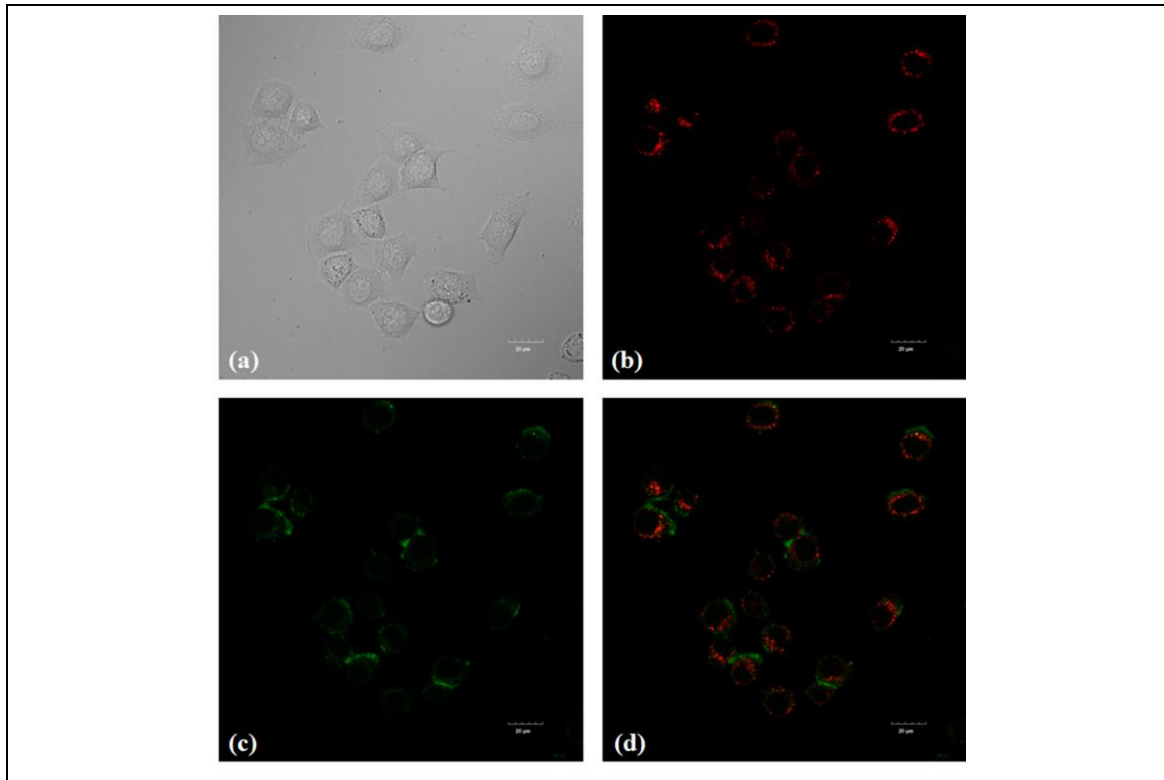


**Figure S19.** Confocal microscopy images of HeLa cells treated with complex **2** (20  $\mu$ M) co-stained with Lysotracker deep red: Panel (a) is bright field; panel (b) is for Lysotracker deep red; panel (c) is for the green fluorescence of complex **2**; panel (d) shows the merged image of (b) and (c) (Scale bar = 20  $\mu$ m; Magnification: 60 X; PCC: 0.40). The PCC value indicates only moderate co-localization in the lysosomes.

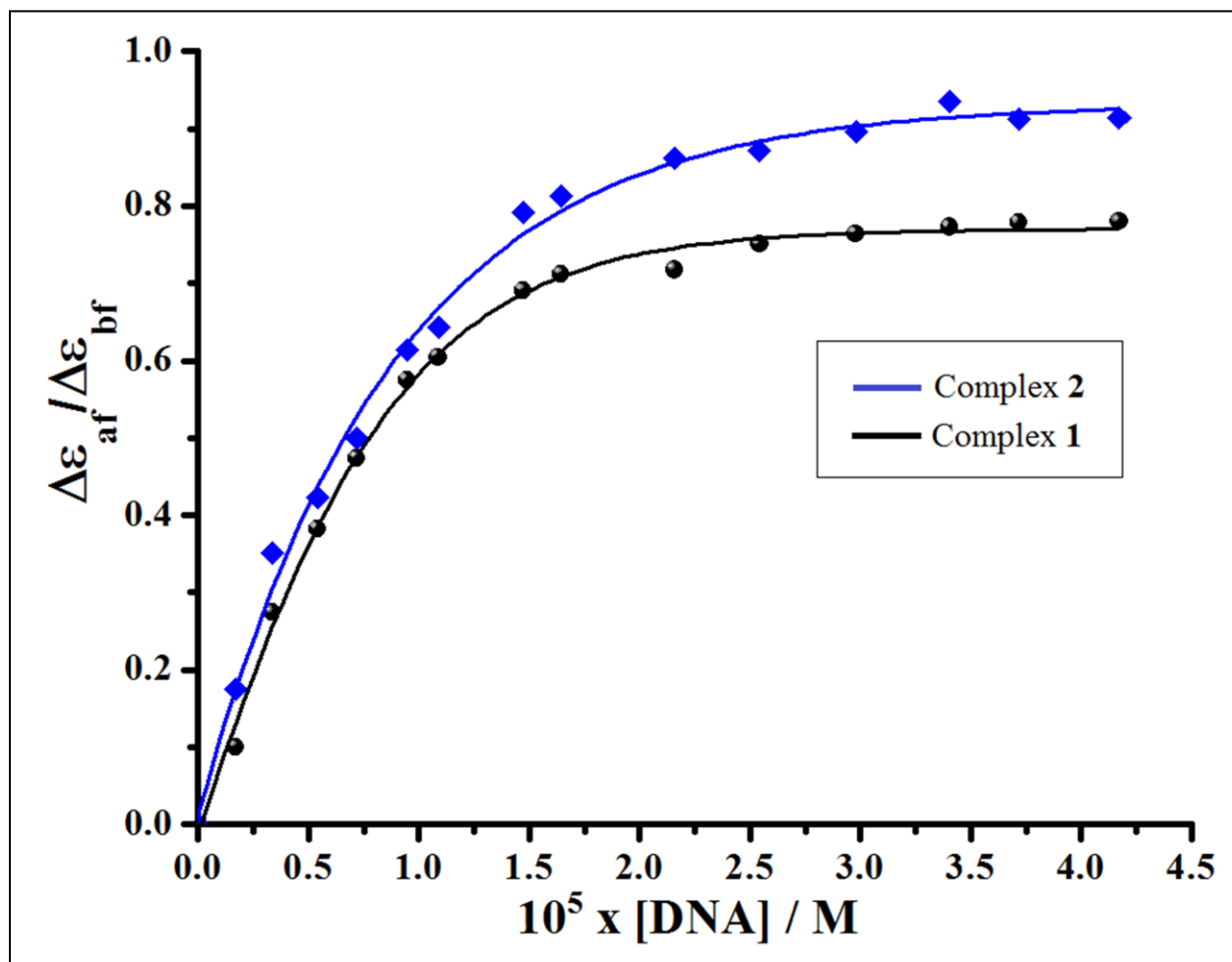


**Figure S20.** The plot of  $\Delta\epsilon_{af}/\Delta\epsilon_{bf}$  vs. [DNA] for the complexes **1** and **2** corresponding to their absorption spectral traces in 5 mM Tris-HCl buffer (pH 7.2) on increasing the quantity of calf thymus DNA.

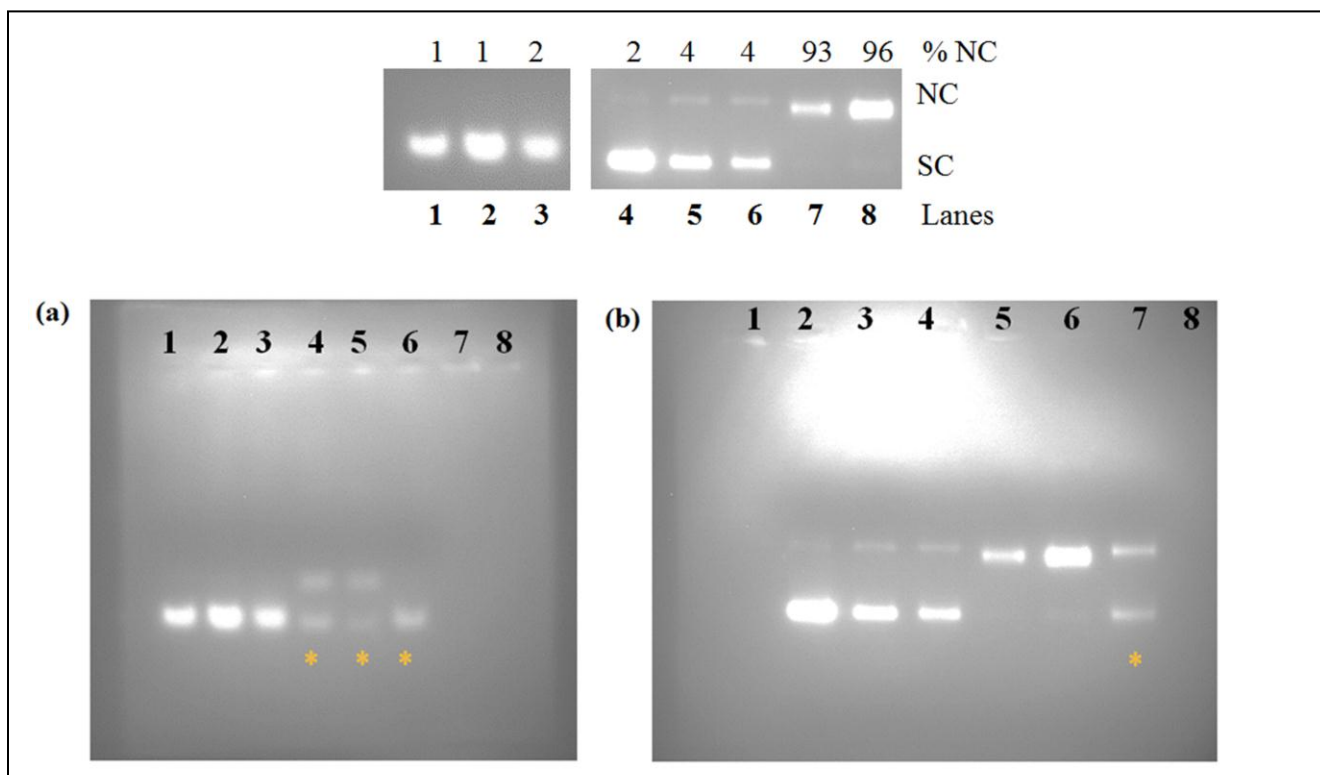


**Figure S21.** Gel electrophoresis diagram showing the cleavage of pUC19 DNA (0.2 mg, 30 mM base pair) by monochromatic light of 446 nm diode laser, where [complex] = 20  $\mu$ M, incubation time: 1 h, exposure time: 1.5 h:

- (a) lane 1: DNA control (Dark); lanes 2 and 3: **1** (Dark) and **2** (Dark);
- (b) lane 2: DNA control (Light); lanes 3 and 4: ligand L<sup>1</sup> (Light) and ligand L<sup>2</sup> (Light); lanes 5 and 6: complex **1** (Light) and complex **2** (Light), where \* means the lanes that were not used for this study.

SC and NC are the supercoiled and the nicked circular form of plasmid DNA.

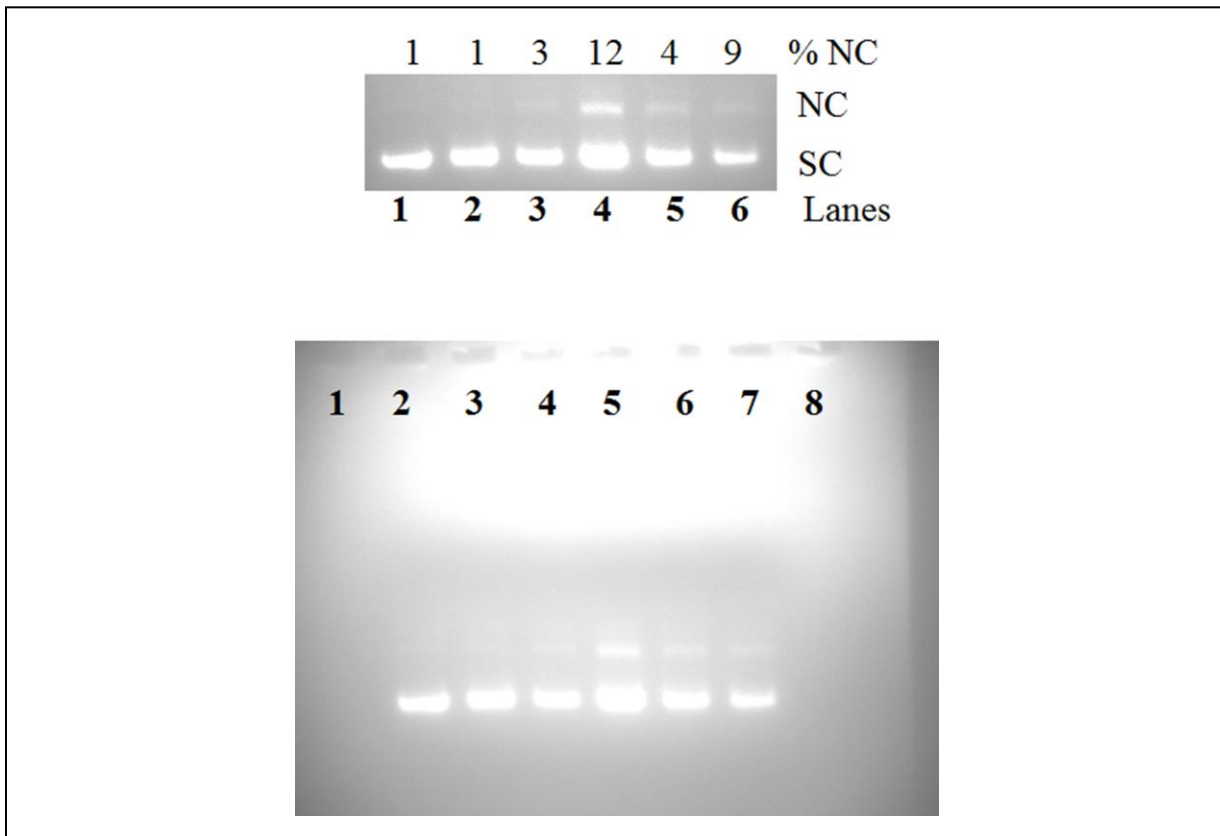


**Figure S22.** Gel electrophoresis diagram showing chemical nuclease activity of the complexes **1** and **2** (20  $\mu$ M) after incubating with GSH/H<sub>2</sub>O<sub>2</sub> (0.5 mM) for 1 h in dark (GSH is glutathione).

(Gel top): The lanes are taken from the raw gel that is shown below with lanes 1-8.

(Gel below): Lane 2: DNA control; lane 3: DNA + GSH; lane 4: DNA + **1** + GSH; lane 5: DNA + **1** + H<sub>2</sub>O<sub>2</sub>; lane 6: DNA + **2** + GSH; lane 7: DNA + **2** + H<sub>2</sub>O<sub>2</sub>.

SC and NC are the supercoiled and the nicked circular form of plasmid DNA.

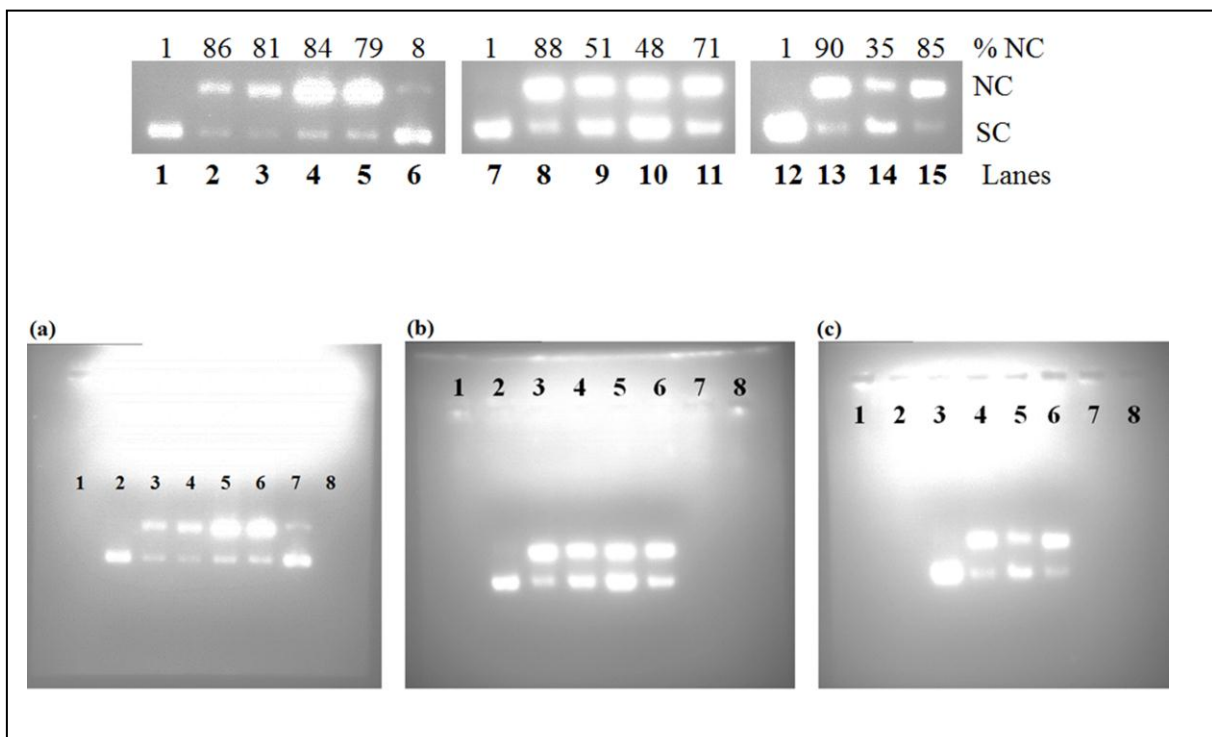


**Figure S23.** Gel diagram showing the mechanistic aspects of photo nuclease activity of complex **2** in the presence of various singlet oxygen quenchers and hydroxyl radical scavengers in monochromatic diode laser light of 446 nm, where [complex] = 20  $\mu$ M, incubation time: 1 h, exposure time: 1 h. The details for the raw gels are given below (**the lanes shown in top are taken from the raw gels shown below**):

- (a) Lane 2: DNA control; lane 3: DNA + **2** (L); lane 4: DNA + **2** + TEMP (0.5 mM); lane 5: DNA + **2** + NaN<sub>3</sub> (0.5 mM); lane 6: DNA + **2** + DABCO (0.5 mM); lane 7: DNA + **2** under argon atmosphere (lanes are all light exposed).
- (b) Lane 2: DNA control; lane 3: DNA + **2** (L); lane 4: DNA + **2** + DMSO (4  $\mu$ L); lane 5: DNA + **2** + KI (0.5 mM); lane 6: DNA + **2** + SOD (superoxide dismutase, 4 units) (lanes are all light exposed).
- (c) Lane 3: DNA control; lane 4: DNA + **2** (L); lane 5: DNA + **2** + catalase (4 units); lane 6: DNA + **2** + D<sub>2</sub>O (16  $\mu$ L) (lanes are all light exposed).

**Table S1:** Computational data for the energy minimized structures of complex **1<sup>[S1]</sup>**

Charge 1

Multiplicity 6

Total Energy -2.163069845046529E+03

Dipole Moment -2.20056736E+00; -2.02004313E+00; -4.26429152E-04

<b>Atomic No</b>	<b>X</b>	<b>Y</b>	<b>Z</b>
7	-2.240844173	-6.930845519	-0.000115000
6	-2.627709202	-5.527734425	-0.000481000
6	-1.387281106	-4.579002349	-0.000119000
6	7.763659593	0.820029062	0.000051000
6	8.082501639	2.241568172	0.000033000
6	6.932873538	3.173463241	0.000043000
6	5.621884424	2.681147204	0.000031000
6	5.354362411	1.291732100	0.000028000
6	6.464026517	0.368107028	0.000048000
6	4.010838304	0.740783055	0.000019000
6	2.828645218	1.436783108	0.000019000
6	1.529309115	0.762243060	0.000024000
6	0.344234026	1.540147115	0.000090000
6	-0.965414071	1.008579075	0.000131000
6	-2.087149160	1.954472147	0.000138000
6	-3.402624258	1.574470118	0.000183000
6	-4.568825349	2.442195185	0.000169000

6	-4.481706343	3.853880295	-0.000101000
6	-5.627934454	4.659243358	-0.000102000
6	-6.973778516	4.046120309	0.000175000
6	-7.020235516	2.590418198	0.000441000
6	-5.874586457	1.827887139	0.000428000
8	9.302295733	2.653725202	0.000016000
8	7.047703519	4.534382345	0.000086000
8	-5.397384415	6.004739454	-0.000340000
8	-8.052988630	4.749082361	0.000186000
8	1.524755117	-0.558086043	-0.000045000
8	-1.221504093	-0.292799022	0.000173000
6	8.332433641	5.266312402	-0.000112000
6	-6.456945490	7.036633554	-0.000661000
7	-1.677588126	-3.083908236	-0.000034000
6	-2.357824180	-2.641081199	1.274433095
6	-1.317005103	-2.461965189	2.365699179
6	-1.574994120	-2.642217200	3.730916282
6	-0.548290041	-2.389582181	4.661647357
6	0.716995055	-1.974729153	4.205229323
6	0.923581070	-1.825127141	2.827326217
7	-0.078797006	-2.058002157	1.946578151
6	-2.357810178	-2.640881202	-1.274443096
6	-1.316985100	-2.461873186	-2.365716182
6	-1.574936122	-2.642212204	-3.730927284
6	-0.548194043	-2.389661182	-4.661642356

6	0.717082052	-1.974796152	-4.205212321
6	0.923632072	-1.825108138	-2.827313215
7	-0.078777006	-2.057905158	-1.946580151
26	0.088252007	-1.916211145	0.000006000
17	1.732475131	-3.651174277	-0.000007000
1	-3.523342268	4.362828331	-0.000334000
1	-8.011092609	2.145303163	0.000647000
1	-5.942561444	0.741928056	0.000628000
1	-3.605267277	0.503583038	0.000254000
1	-1.813710136	3.006916227	0.000113000
1	0.452530035	2.619414201	0.000108000
1	2.806884216	2.523748194	0.000023000
1	3.933163302	-0.346650026	0.000018000
1	8.610939680	0.140452011	0.000062000
1	6.255130464	-0.699270052	0.000059000
1	4.820109368	3.412509263	0.000033000
1	8.031014598	6.315359461	-0.000190000
1	8.914511681	5.018723385	0.890706065
1	8.914342662	5.018550381	-0.890994070
1	-5.901240427	7.975955610	-0.001019000
1	-7.082240537	6.942810534	-0.891601068
1	-7.082159520	6.943434540	0.890399069
1	1.876631142	-1.535184115	-2.401819183
1	1.530730115	-1.781581134	-4.895361373
1	-0.731039055	-2.522768194	-5.723871432

1	-2.554836193	-2.973065230	-4.060449312
1	-2.823347217	-1.669083126	-1.084005085
1	-3.133668239	-3.345258253	-1.591063121
1	-3.257042247	-5.344174426	-0.880989069
1	-3.257830250	-5.343864434	0.879405067
1	-0.764246059	-4.792183367	-0.873295065
1	-0.764658061	-4.792318365	0.873323069
1	-3.133519238	-3.345646257	1.591040123
1	-2.823581213	-1.669368130	1.084105083
1	1.530619115	-1.781452137	4.895389372
1	-0.731169057	-2.522617194	5.723879422
1	-2.554897196	-2.973071225	4.060430309
1	1.876591141	-1.535218115	2.401846182
1	-1.877039143	-7.331405550	-0.854890063
1	-1.877310145	-7.331043540	0.854947066

**Table S2:** Computational data for the energy minimized structures of complex **2**

Charge 1

Multiplicity 6

Total Energy -2.823882612948552E+03

Dipole Moment 2.20387029E+00; -7.94783954E-01; 7.94519377E-01

<b>Atomic No</b>	<b>X</b>	<b>Y</b>	<b>Z</b>
7	-6.471773460	2.291346564	-2.316057247
6	-7.921097498	2.063496006	-2.159107857
6	-8.091835214	0.630281304	-2.800945397
7	-6.860208876	0.506610102	-3.590950218
6	-5.872618076	1.406306034	-3.205698676
6	-8.411376674	2.071389965	-0.690313732
6	-8.258042486	-0.438691483	-1.667683436
16	-9.366939444	0.451555543	-0.399384415
8	-4.668571234	1.401931812	-3.568424947
6	-6.921416850	-0.913241444	-1.072150149
6	-6.997353468	-2.005950975	0.014635071
6	-5.560283905	-2.340312398	0.466882058
6	-5.426765130	-3.467191836	1.524220039
6	-3.941876195	-3.689177760	1.783346178
7	-3.442583348	-3.245412683	2.988209796
8	-3.175259226	-4.174842341	0.900489886
6	-1.997653333	-3.214697526	3.254288149
6	-1.336773810	-1.872274838	2.788393123
6	2.148596894	7.994138246	0.734664866
6	3.215933176	8.471522748	-0.036135148
6	4.080995629	7.552767537	-0.700520085
6	3.877311560	6.179886434	-0.591677040
6	2.793107795	5.682250636	0.191318074

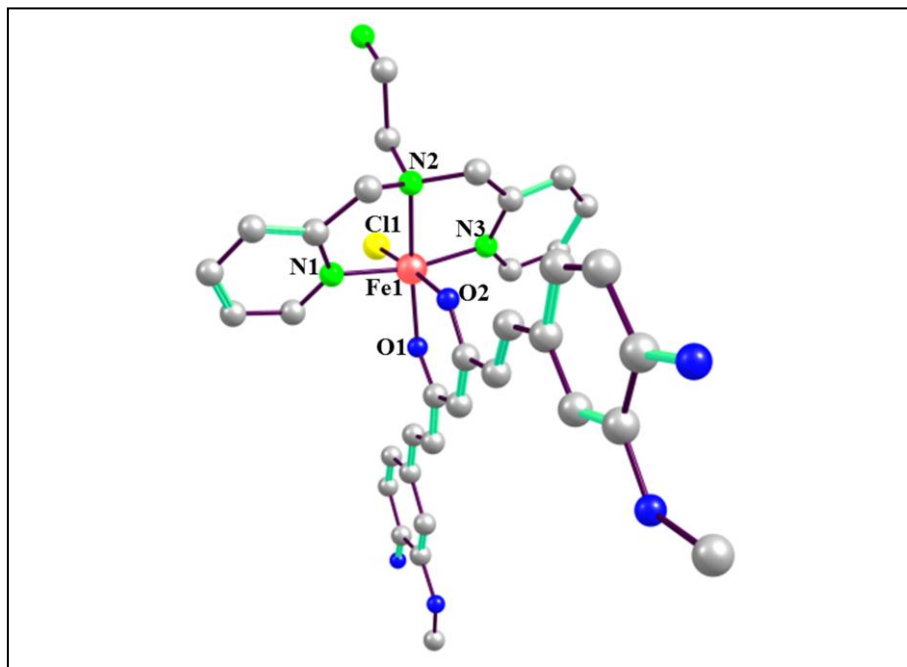
6	1.942558663	6.611819849	0.844430393
6	2.515426548	4.263961531	0.352522203
6	3.200713567	3.201450029	-0.178614133
6	2.793741824	1.827783848	0.072785124
6	3.513986663	0.749807040	-0.484734727
6	3.185393018	-0.616736520	-0.295619376
6	4.030647542	-1.625692867	-0.932282141
6	3.802500348	-2.970280598	-0.833483838
6	4.573982393	-4.059551997	-1.418195927
6	5.740627089	-3.845072431	-2.210002246
6	6.432039075	-4.933106353	-2.737165960
6	5.986539355	-6.265463444	-2.494207900
6	4.842102974	-6.487556119	-1.719045031
6	4.146077123	-5.391900022	-1.188243081
8	3.430792151	9.828219600	-0.153570997
8	5.090462341	8.194389183	-1.424377765
8	7.584214054	-4.888294830	-3.526539631
8	6.681505084	-7.333064097	-3.021867797
8	1.721933026	1.633520854	0.844506288
8	2.148675408	-1.011597063	0.433156796
7	-0.112543077	-2.007457882	1.917770567
6	-0.433229028	-2.584803601	0.564377114
6	-1.063826768	-1.525962382	-0.320287691
6	-2.012142344	-1.831806082	-1.309823855
6	-2.515162520	-0.793395666	-2.114899707

6	-2.073606689	0.528512640	-1.906580352
6	-1.133550474	0.767147972	-0.895464602
7	-0.642859805	-0.244937111	-0.130733566
6	1.013068938	-2.705012711	2.615137909
6	1.682298550	-1.772439994	3.609071474
6	2.286780896	-2.215557835	4.796210141
6	2.937643951	-1.280620521	5.622780479
6	2.956584226	0.076522363	5.248539926
6	2.321640934	0.455541162	4.056956880
7	1.710640384	-0.457265392	3.261695292
26	0.732315610	0.077457451	1.438999382
17	-0.795691745	1.429378691	2.632620041
1	7.455980171	-7.017977146	-3.540643829
1	4.518560602	-7.508734645	-1.547571573
1	3.256233008	-5.568650462	-0.588337916
1	6.089086814	-2.835640480	-2.400896906
1	1.113487761	6.241268772	1.442361785
1	4.539995942	5.488882707	-1.102087886
1	1.502379910	8.709764431	1.231686490
6	8.165674438	-3.594796405	-3.869447150
6	6.058280973	7.391471983	-2.163513575
1	9.039841862	-3.821407127	-4.481514961
1	7.453688146	-2.990315953	-4.446552622
1	8.474793910	-3.056242971	-2.964003286
1	6.730383176	8.108234576	-2.637634673

1	6.625511093	6.743496558	-1.482393753
1	5.556295020	6.787913739	-2.931106040
1	4.212988120	10.005155305	-0.723816330
1	4.870821942	-1.240876399	-1.505622025
1	4.376106864	0.982514196	-1.100794122
1	4.074633363	3.338280655	-0.811108647
1	2.935588262	-3.272755705	-0.246211084
1	1.654303375	4.012702072	0.972548222
1	3.439828911	0.826112775	5.865709509
1	3.413358164	-1.603145635	6.544461406
1	2.249879605	-3.266758089	5.065744906
1	-5.997555502	3.137140366	-2.031890588
1	-6.661074397	-0.244025491	-4.236190621
1	-9.099298683	2.893987347	-0.482931160
1	-6.305776854	-1.303843353	-1.896630385
1	-6.377228589	-0.047777483	-0.668523928
1	-7.487798223	-2.906905590	-0.385501657
1	-7.602318371	-1.656855581	0.862406550
1	-5.854358921	-4.397234938	1.131627084
1	-5.965727554	-3.205435945	2.444465927
1	-4.079000430	-2.865601316	3.678748058
1	-1.557158994	-4.070690416	2.732069867
1	-1.843694928	-3.360774625	4.328983477
1	-1.059888456	-1.257679306	3.648671438
1	-2.069069703	-1.291771032	2.222469573

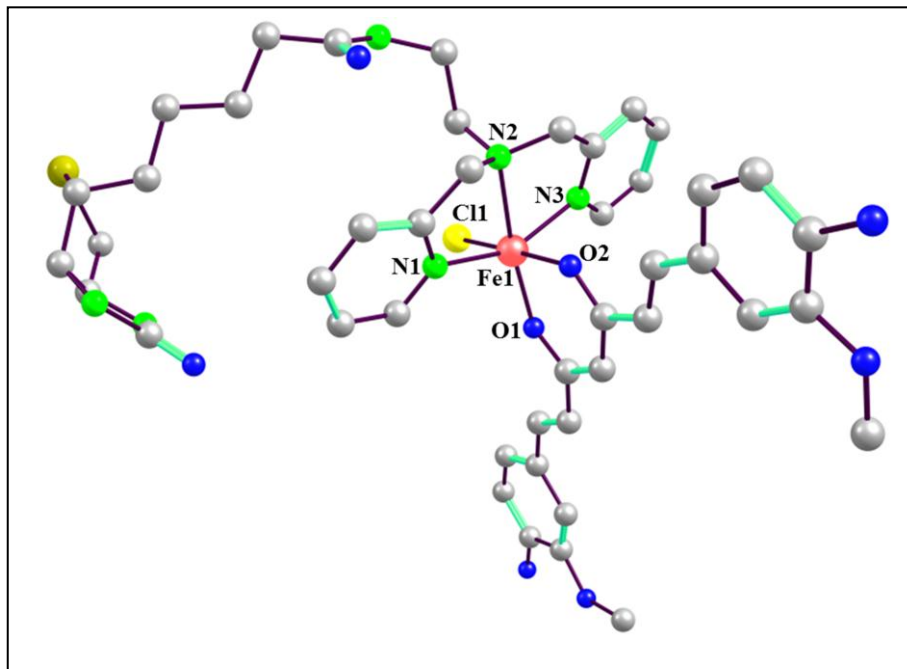
1	-1.106918994	-3.446640005	0.634545472
1	0.512285914	-2.896050233	0.107901714
1	1.754394849	-2.973641080	1.855612677
1	0.688245999	-3.626825752	3.115642826
1	-8.491525066	2.796829690	-2.744009836
1	-8.980929406	0.604304051	-3.437458462
1	-4.970024208	-2.639048624	-0.409757077
1	-5.095315288	-1.423093764	0.861889882
1	2.280111914	1.487572430	3.727517155
1	-0.771171291	1.762959958	-0.666087363
1	-2.487084746	1.335889793	-2.500893033
1	-3.254947028	-0.986131720	-2.885428164
1	-2.357689251	-2.854973717	-1.416534686
1	-8.846677402	-1.290673788	-2.028772374
1	-7.567545288	2.116078317	0.002651627

**Table S3: Estimated Bond Distances [Å] and Angles [°] for the Complex 1 from the DFT Calculations**



Bond	Bond Length (Å)	Bond	Bond Angle (°)
Fe(1)-O(1)	1.9769	N(1)-Fe(1)-O(1)	96.41
Fe(1)-O(2)	2.0858	O(1)-Fe(1)-O(2)	85.50
Fe(1)-N(1)	1.9588	Cl(1)-Fe(1)-O(2)	175.43
Fe(1)-N(2)	2.117	Cl(1)-Fe(1)-N(2)	99.98
Fe(1)-N(3)	1.9588	N(1)-Fe(1)-N(3)	167.16
Fe(1)-Cl(1)	2.3903	O(1)-Fe(1)-N(2)	170.08
		N(3)-Fe(1)-O(2)	90.16

**Table S4: Estimated Bond Distances [Å] and Angles [°] for the Complex 2 from the DFT Calculations**



Bond	Bond Length (Å)	Bond	Bond Angle (°)
Fe(1)-O(1)	1.9376	N(1)-Fe(1)-O(1)	103.13
Fe(1)-O(2)	2.0503	O(1)-Fe(1)-O(2)	85.6
Fe(1)-N(1)	2.1116	Cl(1)-Fe(1)-O(2)	176.45
Fe(1)-N(2)	2.2999	Cl(1)-Fe(1)-N(2)	100.13
Fe(1)-N(3)	2.1366	N(1)-Fe(1)-N(3)	153.39
Fe(1)-Cl(1)	2.3637	O(1)-Fe(1)-N(2)	168.38
		N(3)-Fe(1)-O(2)	88.24

## References

[S1] M. J. Frisch, G. W. Trucks, H. B. Schlegel, G. E. Scuseria, M. A. Robb, J. R. Cheeseman, G. Scalmani, V. Barone, B. Mennucci, G. A. Petersson, H. Nakatsuji, M. Caricato, X. Li, H. P. Hratchian, A. F. Izmaylov, J. Bloino, G. Zheng, J. L. Sonnenberg, M. Hada, M. Ehara, K. Toyota, R. Fukuda, J. Hasegawa, M. Ishida, T. Nakajima, Y. Honda, O. Kitao, H. Nakai, T. Vreven, J. A. Montgomery Jr., J. E. Peralta, F. Ogliaro, M. Bearpark, J. J. Heyd, E. Brothers, K. N. Kudin, V. N. Staroverov, R. Kobayashi, J. Normand, K. Raghavachari, A. Rendell, J. C. Burant, S. S. Iyengar, J. Tomasi, M. Cossi, N. Rega, J. M. Millam, M. Klene, J. E. Knox, J. B. Cross, V. Bakken, C. Adamo, J. Jaramillo, R. Gomperts, R. E. Stratmann, O. Yazyev, A. J. Austin, R. Cammi, C. Pomelli, J. W. Ochterski, R. L. Martin, K. Morokuma, V. G. Zakrzewski, G. A. Voth, P. Salvador, J. J. Dannenberg, S. Dapprich, A. D. Daniels, Ö. Farkas, J. B. Foresman, J. V. Ortiz, J. Cioslowski, D. J. Fox, Gaussian 09, Revision A.02, Gaussian, Inc., Wallingford CT, 2009.